Modeling the Process of Drying Biomass in a Fixed Bed

Hai Yang
Michael R. Milota

Abstract

An alternative to a rotary dryer for biomass is a bed dryer. In this type of dryer, the wood particles are stationary, and the air passes upward through them. Compared with rotary dryers, bed dryers may be more economical to operate on a small scale. The present work investigated drying biomass in a fixed bed dryer.

The drying characteristics of wood biomass were measured using a thin-layer drying technique at inlet gas conditions of 50°C to 200°C and 0.3 to 0.9 m/s. The drying behavior was modeled using a one-parameter Newton model. The thin-layer model was then used in a deep bed model to predict drying times and moisture profiles in the bed. Drying times based on the model at depths up to 23 cm were within −22 to +12 percent, and typically within ±4 percent, of the experimental results.

A drying zone ranging from 0.13 to 0.18 m in depth moves up the bed as drying occurs. The biomass is wet above and dry below this zone, resulting in considerable variability in moisture content within the bed. The material in an industrial dryer would need to be mixed or a dryer would need to be designed with stages if a uniform moisture content among the particles was an important criterion.

Drying is often an important step to convert biomass into bioproducts (Phanphanich and Mani 2009). A moisture content of 20 percent is needed for some gasifiers and an even lower value for pelletization (Roos 2008). Even for direct incineration, lower moisture content can lead to greater efficiency and fewer emissions (Jackson et al. 2010).

The most common type of dryer for wood and bark residues is the rotary dryer in which particles are fed through a rotating drum, often with concurrent airflow. An alternative to the rotary dryer is a bed dryer in which air passes upward through a layer, or bed, of biomass. The bed might be stationary, as in some batch agricultural applications, or it might be moving on a conveyer, as in a continuously fed dryer. For small particles (<6 mm), a spouting bed may be used; this type of dryer contains a central jet that carries the particles upward surrounded by an annulus of downward-moving particles (Cui and Grace 2008). A fluidized bed (Milota and Wilson 1990) could be used for very small (<3-mm) particles that are not elongated. Forest biomass produced with a hog or grinder tends to have a wide size distribution and particles with very nonspherical or elongated shapes. This can cause feed problems in the airlocks of a rotary dryer, particularly in a small-scale operation, and poor flow in a spouted or fluidized bed.

The air entering a bed dryer is typically lower in temperature than for a rotary dryer, making the bed dryer more suitable for recovering low-grade heat and reducing the chance of fire. For example, Yrjölä and Saastamoi (2002) describe a heat recovery system in which the drying air is heated in a recuperative heat exchanger using the boiler flue gases. The bed dryer will have lower organic emissions due to the lower operating temperature (Otwell et al. 2000) and may also have lower particulate emissions because the biomass is not mixed, resulting in less breakage. This may reduce the capital and operating costs compared with a rotary dryer, partly because less pollution control equipment may be needed (Jackson et al. 2010). The moisture content leaving a bed dryer is not as uniform as with a rotary dryer (Wang and Chen 1999); however, mixing the biomass or several drying stages could resolve this. Bed dryers have a larger footprint than a rotary dryer of comparable productivity, but this can be reduced with a multiple-pass arrangement.

Models for bed dryers are often developed by determining the drying behavior of individual particles and then using a mathematical technique to predict the behavior for a deeper bed. The particle drying characteristics could be fit to an

The authors are, respectively, Graduate Student and Professor, Wood Sci. and Engineering, Oregon State Univ., Corvallis (Hai.Yang@OregonState.edu, Mike.Milota@OregonState.edu [corresponding author]). This paper was received for publication in June 2013. Article no. 13-00054.

Forest Prod. J. 63(5/6):148–154.
doi:10.13073/FPJ-D-13-00054

empirical model (Gigler et al. 2000) or a theoretical model (Wang and Chen 1999).

In this article, we determine the drying characteristics of Douglas-fir and hemlock biomass in a batch fixed bed dryer. The objectives were to determine the effect of gas temperature and velocity on the drying rates and to develop a model to simulate bed drying. Drying curves were first determined by drying a thin layer of wood so that temperature change through the layer was minimal and all the wood was exposed to essentially the same conditions. Experiments were then done to determine the drying rate and temperature profile in a deeper bed. Finally, a model was developed using the drying curves from the thin-layer experiments to predict behavior in the deeper bed, and the results were compared with the deep bed measurements.

Procedures

The biomass used in this study was western hemlock (*Tsuga heterophylla*) and Douglas-fir (*Pseudotsuga menziesii*) wood chips sampled from outdoor storage piles. Material was taken from the inside of the piles and stored in 20-gallon plastic containers for up to 2 weeks at 5°C or in a freezer at –5°C for longer-term storage.

Size distribution of the material was determined by screening material from four randomly selected containers into those smaller than ⅜ inch, those from ⅜ to 2 inches, and those larger than 2 inches (<10, 10 to 50, and >50 mm, respectively) and weighing the fractions. The moisture contents of four 120-g samples were used to determine initial moisture content by ASTM D4442 (ASTM International 2007). Starting and ending moisture contents were also determined for each drying experiment using this method.

A 42-cm-diameter batch bed dryer was direct-fired with natural gas (Fig. 1). Gas was supplied to the dryer from a New York Blower 1804S pressure blower controlled with a Toshiba variable-frequency drive. A Power Flame FD75 natural gas burner controlled by a Honeywell Modutrol IV motor was located at the blower intake. Combustion gas from the burner was combined with ambient air and went to the blower intake and to a duct with a Y-connection. The Y-connection allowed the air to go to or bypass the dryer so that the burner and blower could be run at steady conditions while the dryer was being loaded or unloaded. At the base of the dryer, the duct made a 90° turn and expanded to 46 cm. There were two perforated plates to make the airflow uniform across the bed cross section. The open area of the perforated plates was 33 percent.

The dryer walls are square in cross section, 56.5 cm on a side, and 125 cm in height. The bottom of the dryer had a 46-cm-diameter hole to which the ductwork from the blower was attached.

A basket 42 cm in diameter and 56 cm in height had a circumferential flexible gasket at its base to seal the gap between the basket and dryer structure. The basket rested on four rods that passed though the bottom of the dryer and were supported by load cells, allowing the basket and wood to be continually weighed with the load cells outside the heated space.

Thermocouples were used to measure temperature under the perforated plates, in the bed at three locations, and at the dryer exit. Pressure was measured below the distributor plates, below the basket, and above the basket. The differential pressure across the basket and its area were used to adjust the measured basket weight for the lifting force caused by the gas pressure. The pressure transducers were located outside the dryer and connected to small copper tubes that terminated at the measurement location.

The blower and burner were computer controlled with Labview software. The software also recorded all temperatures and pressures. Additional experimental details can be found in Yang (2012).

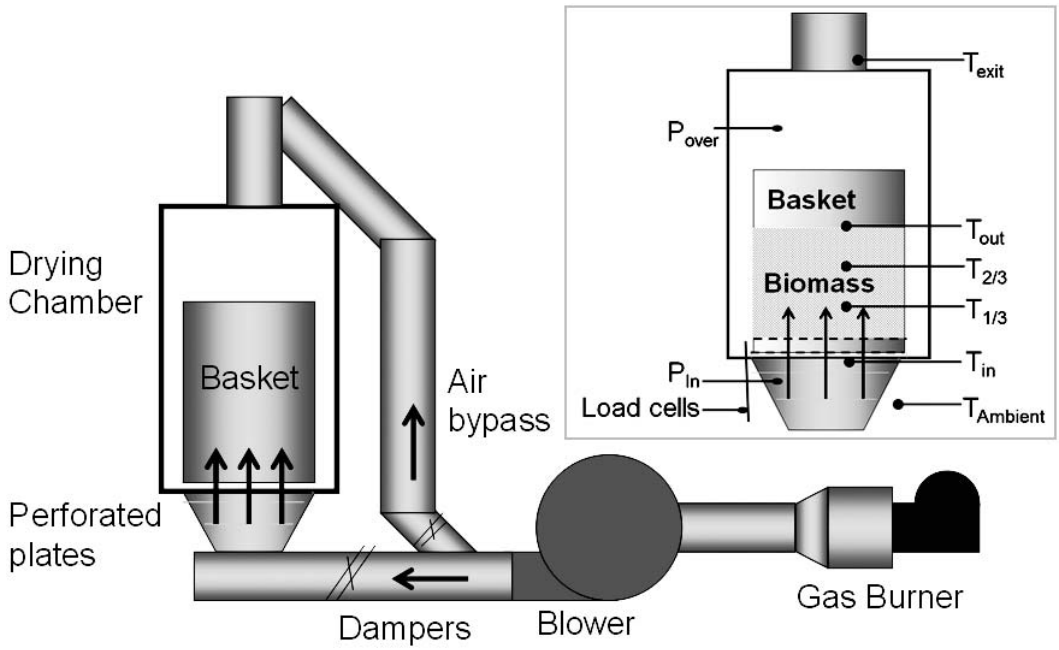

Figure 1.—Schematic of drying equipment. T and P indicate locations where temperature and pressure, respectively, were measured.

Thin-layer drying

Thin-layer drying of hemlock was conducted at a depth of approximately 1.3 cm so that little temperature change occurred throughout the bed depth. All the biomass was exposed to approximately the same gas temperature and velocity. Drying curves were then constructed for temperatures of 50°C, 100°C, 150°C, and 200°C and air velocities of 0.3, 0.6, and 0.9 m/s. Three replications were done at each of the 12 conditions.

A 50- to 100-g sample of material to be dried was taken to determine initial moisture content (M_I). The dryer was brought to a steady-state temperature with the empty basket in the dryer. The basket was then loaded with 800 g of wood in a thin layer. At regular intervals, a sample of approximately 50 g of material was removed from the bed, and the material remaining in the bed was leveled. The removed material was weighed and its moisture content determined. The time intervals for sample collection ranged from 30 seconds to 10 minutes, depending on the dryer conditions and drying time. Samples were closely spaced in time early in the drying process and for higher temperatures. From the initial moisture content and the current moisture content (M), the relative moisture content (M_R) was determined for each 50-g sample as

$$M_R = \frac{M - M_E}{M_I - M_E} \quad (1)$$

where M_E is the equilibrium moisture content (US Department of Agriculture 2010) with the humidity values based on a stoichiometric calculation on the incoming gas. Volatilization of wood components would appear as moisture loss. However, the samples contained moisture when taken and were cooled by evaporation during drying, so significant volatilization was unlikely.

Ten models from the literature (of the 14 models summarized in Ertekin and Yaldiz 2004; Table 1) were fit to the drying curves. Time was the independent variable, and relative moisture content was the dependent variable. The average root mean square error and adjusted r^2 for all the thin-layer hemlock drying experiments were used as the primary criteria to select the best model to predict the drying rates. Having fewer parameters was also considered to be a positive property of a robust model. The model coefficients, which vary with drying conditions, were then fit to the air temperature and velocity with a second regression using the equations in Table 2.

Table 2.—Equations and parameters tested to fit k *to gas temperature and velocity.*

	Equation/model parameter[a]	r^2	RMSE[b]
1	$k = -e^{\frac{b}{T}} \cdot a\sqrt{V} + c$ $a = 11.46,\ b = -1{,}583.41,\ c = 0.016$	0.90	0.03
2	$k = a \cdot e^{\frac{b}{T}}$ $a = -4.24,\ b = 1{,}366.48$	0.63	0.07
3	$k = a \cdot T^2 + b \cdot V + c$ $a = 0,\ b = -0.15,\ c = 0.28$	0.83	0.05
4	$k = a \cdot T + b \cdot V + c \cdot T \cdot V$ $a = 0,\ b = 0.91,\ c = -0.003$	0.92	0.03
5	$k = a \cdot T + b \cdot V + c$ $a = -0.002,\ b = -0.15,\ c = 0.62$	0.84	0.05

[a] Terms are defined in the article text and Table 1.
[b] RMSE = root mean square error.

Bed drying

The dryer, including the basket, was preheated to a steady-state condition matching the experiment to be performed. Most experiments were done with hemlock, but for a limited set, we used Douglas-fir. The initial moisture content was determined from three 100- to 200-g samples of the material to be used for the experiment.

The airflow was set to bypass the dryer, and the basket was removed, loaded, and weighed. If used, thermocouples were placed at ⅓ and ⅔ of the depth as well as at the surface of the bed. The basket was returned to the bed, the dampers reset, and the drying started. Steady-state conditions of 50°C, 100°C, 150°C, or 200°C and an air velocity of 0.3, 0.6, or 0.85 m/s were held until the bed approached dryness, as evidenced by the bed weight. Air velocities were less than 0.9 m/s because significant particle entrainment started to occur at this velocity. Three replications were done at each combination of temperature and air velocity.

At the end of drying, the basket with biomass was weighed, and three 500-g samples were used to determine the final moisture content. Moisture content at any time was calculated from the load cell weight data.

Model

A bed drying model was developed to predict the performance of the deep bed from the model representing thin-layer drying. The model divides the bed into layers (0.5-cm layers were used). The drying air enters the bottom layer, and the thin-layer drying model is used to obtain a

Table 1.—Models from Ertekin and Yaldiz (2004) tested to create drying curve for thin-layer drying.

	Name	Model[a]	Adjusted r^2	RMSE[b]
1	Newton	$M_R = e^{-kt}$	0.97	0.06
2	Henderson and Pablis (1962)	$M_R = a \cdot e^{-kt}$	0.16	0.32
3	Logarithmic	$M_R = a \cdot e^{-kt} + c$	0.36	0.28
4	Two-term	$M_R = a \cdot e^{-k_0 t} + b \cdot e^{-k_1 t}$	0.07	0.33
5	Two-term exponential	$M_R = a \cdot e^{-kt} + (1 - a)e^{-kat}$	0.16	0.31
6	Wang and Singh (1978)	$M_R = 1 + a \cdot t + b \cdot t^2$	0.97	0.60
7	Paulsen and Thompson (1973)	$t = a \cdot \ln(M_R) + b(\ln(M_R))^2$	0.92	1.52
8	Diffusion approximation	$M_R = a \cdot e^{-kt} + (1 - a)e^{-kbt}$	−0.57	0.43
9	Verma et al. (1985)	$M_R = a \cdot e^{-kt} + (1 - a)e^{-gt}$	0.99	0.03
10	Modified Henderson and Pablis	$M_R = a \cdot e^{-kt} + b \cdot e^{-gt} + c \cdot e^{-ht}$	0.99	0.04

[a] Terms are defined in the article text. *a, b, c, d, e, f,* and *g* are empirical coefficients.
[b] RMSE = root mean square error.

drying rate based on the temperature, humidity, and velocity at entry. A new moisture content is calculated for the layer. The gas humidity leaving the layer is calculated by a mass balance and its temperature by an energy balance using the process calculations in Chapter 3 of Mujumdar (2007). Air at the new temperature, humidity, and velocity enters the second layer, and the calculations are repeated to the top of the bed. The bed drying model can predict drying time or final moisture content given other parameters such as initial moisture content, air temperature at entry, and air velocity at entry. The moisture content and gas temperature for any bed location can also be predicted at any time.

Results and Discussion

The hemlock was uniform in size, with 95 percent of the wood chips in the medium class (⅜ to 2 in.), 4.5 percent in the small class (<⅜ in.), and 0.5 percent in the large class (>2 in.). The uniform size was a result of prescreening at the mill. The average initial moisture content was 159.8 percent (±2.3%). The Douglas-fir had been across the same screen and had a similar size distribution with an initial moisture content of 92 percent.

Thin-layer drying

An increase in temperature greatly reduces drying time (Fig. 2). For example, increasing the temperature from 50°C to 100°C reduced the drying time from green to 10 percent moisture content at the low velocity by a factor of approximately 2.32, while increasing the temperature from 150°C to 200°C reduced drying time by a factor of 1.43. One would expect factors of 2.22 and 1.62 for the experimental value $H = 16{,}000$ J/mol if drying is mostly controlled by internal diffusion (D) and based on the Arrhenius relationship

$$D \approx \mathbf{e}^{-H/RT} \tag{2}$$

where H is the activation energy, R is the gas constant (8.316 J/mol/K), and T is the absolute temperature (K). Published values for H are 35,564 J/mol (Skaar 1998) to 40,000 J/mol (Siau 1984). There are several possible reasons why the experimental value is different. The mechanism for moisture movement in the small particles may be only partially diffusion controlled. At the higher temperatures, the internal water may evaporate rapidly, and wood permeability may control the rate. In addition, the published values are for a lower temperature (25°C) than used in the dryer for this study, and the wet-bulb depression and equilibrium moisture content are somewhat different at each of the four drying conditions, which changes the driving force for diffusion in addition to affecting the change in diffusion coefficient.

An increase in gas velocity increased the drying rate (Fig. 2) at 100°C, 150°C, and 200°C, but the effect of velocity appeared to be small at 50°C. Greater velocity increases convective heat transfer from the surrounding gas to evaporate surface moisture (Mujumdar 2007). This suggests that at 50°C, the drying rate is mostly limited by internal diffusion. At 200°C, the drying times to 10 percent moisture

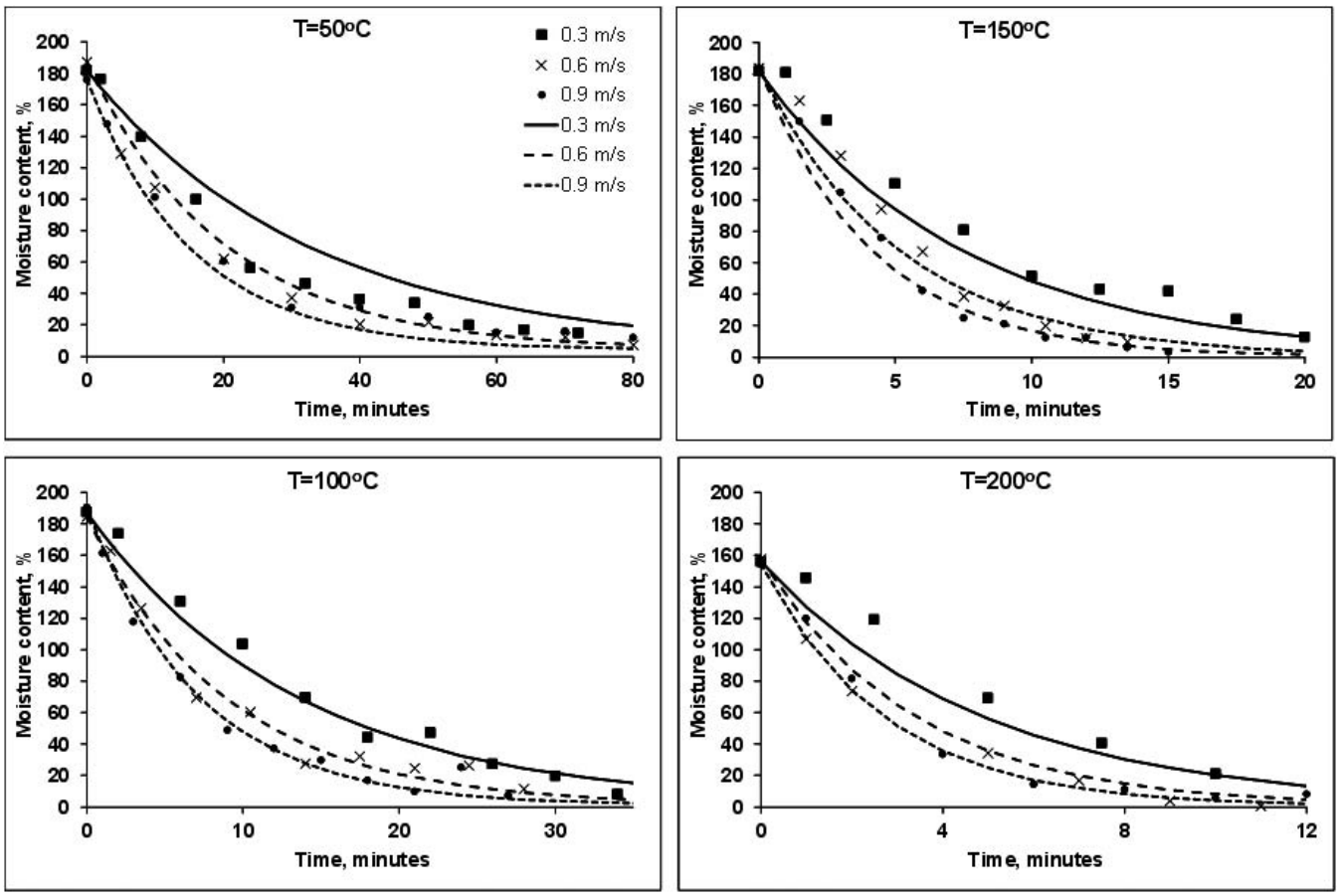

Figure 2.—Thin-layer drying data from one replication (points) and results of modeling based on all replications (lines).

content (13.0, 8.0, and 6.8 min) change by factors of 1.62 from 0.3 to 0.6 m/s and 1.17 from 0.6 to 0.9 m/s. This is in approximate agreement with the theory that heat transfer increases with the square root of velocity. Perfect agreement would mean factors of 1.41 and 1.22, respectively. This indicates that drying rate is externally controlled at higher temperatures.

Of the 10 models from Ertekin and Yaldiz (2004) that were tested (Table 1), the Newton (Westerman et al. 1973), Verma et al. (Verma et al. 1985), Wang and Singh (1978), and modified Henderson and Pablis (Henderson and Pablis 1962) models provided good fits with average adjusted r^2 values of 0.97 or greater. The Verma et al. model, however, has three parameters, while the modified Henderson and Pablis model has six. The Newton model was selected for further study for several reasons: It fits well, has only one parameter, conforms to drying theory for the falling rate period, and has been widely used in many drying applications, including for wood.

Mujumdar (2007) suggests Equation 3 for biological materials, where k embodies diffusion, thermal conductivity, and interface heat and mass transfer and t is time:

$$\frac{dM}{dt} = k \cdot (M - M_E) \quad (3)$$

the solution of which has a form matching the Newton model:

$$\frac{M - M_E}{M_I - M_E} = e^{kt} \quad (4)$$

The parameter k changes as the drying conditions change and needs to be expressed as a function of temperature and gas velocity. Each model in Table 2 was fit to the values for k obtained at each condition of air temperature and velocity at entry. The models represent either a linear combination of the drying variables or an $e^{1/T}$ form for temperature and a square root relationship for velocity. Model 4 had the best fit; however, Model 1 was selected because it contained terms that matched drying theory—an Arrhenius-type term for temperature and a square root term for velocity. The values for k predicted by the model with $a = 11.46$, $b = 1{,}581.41$, and $c = 0.016$ are shown in Table 3. When the equation for k is substituted into Equation 4, the drying curve is described as

$$M = (M_I - M_E) \cdot e^{-(11.46e^{\frac{1{,}581.41}{T}} \cdot \sqrt{V} + 0.016)} + M_E \quad (5)$$

for particles exposed to a certain temperature (T; K) and gas velocity (V; m/s). The lines in Figure 2 show the model predictions using Equation 4 compared with the experimental results and indicate that the model predicts k well at air velocities of 0.3 and 0.6 m/s and also at 0.9 m/s if the temperature is high. The average difference between the k values predicted by Equation 4 and those fit directly to the data for a given experiment is 6 percent at 0.3 m/s, 2 percent at 0.6 m/s, and 19 percent at 0.9 m/s. The predictions were better at 100°C, 150°C, and 200°C than at 50°C. The average difference between the model and the experiment is 19 percent at 50°C and ranges from 4 to 11 percent at 100°C to 200°C.

Table 3.—Values for k *predicted from the model.*

	Temperature (°C)			
Velocity (m/s)	50	100	150	200
0.3	−0.031	−0.074	−0.133	−0.205
0.6	−0.050	−0.111	−0.194	−0.296
0.9	−0.065	−0.140	−0.241	−0.366

Bed drying

Figure 3 shows the relationship between moisture content and time during bed drying. After a short warm-up period in which bed conditions stabilize, the curves are mostly linear until 15 to 30 percent moisture content is reached, and then they become asymptotic to equilibrium moisture content as time becomes long. The linear portion is due to the gas in the bed reaching saturation before exiting the bed rather than being affected by the drying characteristics of the biomass. Higher temperatures result in faster drying in this region because the adiabatic saturation temperature of the air is higher and it can carry more water from the bed. Higher velocities in this region result in faster drying because more air is available to carry the water. The nonlinear portion begins when the air leaving the bed is no longer saturated.

Saturation of the air occurs over a portion of the bed, as illustrated by temperature measurements at various bed depths (Fig. 4). The temperature at ⅓ the bed depth ($T_{1/3}$ in Fig. 4) starts rising at approximately 25 minutes and approaches the temperature at the inlet (Fig. 4) at approximately 95 minutes. Before 25 minutes, the air reaching this depth is saturated, and the temperature is near the adiabatic saturation temperature. At 25 minutes, the wood at this point begins to dry, and at 95 minutes, it is dry. Thus, there is a drying zone below which the wood in the bed is dry and above which no drying has occurred because the air is saturated. A similar trend is seen for the temperature at ⅔ of the bed depth.

The speed at which this drying zone moves and its thickness are of interest in dryer design. These can be determined for any drying condition using the curves in Figure 3. The top of the drying zone is near the distributor plate at the beginning of the linear portion ($t = 0$). The top of the drying zone is at the top of the bed at 120 minutes (t_{top}) for the case shown in Figure 3. A close approximation to the drying zone velocity (V_{dz}) can be expressed as

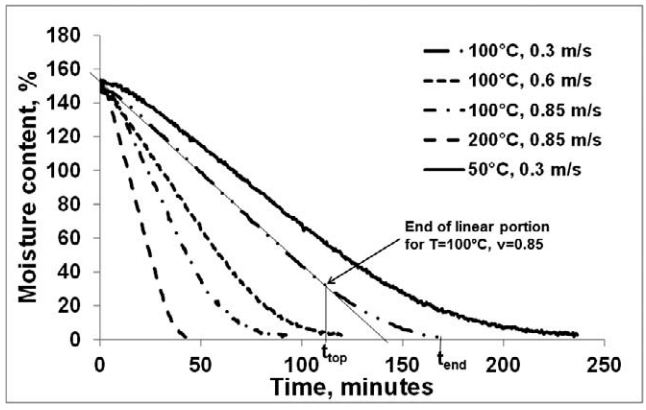

Figure 3.—Experimentally determined curves for moisture content versus time from drying hemlock in a 23-cm-deep bed under a range of conditions.

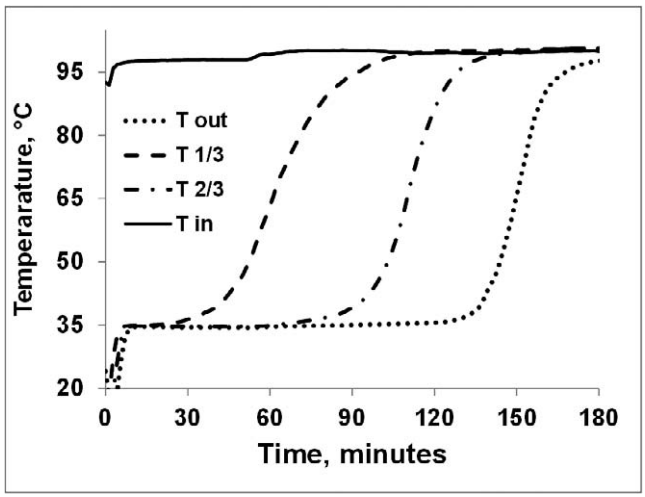

Figure 4.—Temperatures at the inlet and at different heights for drying in a 23-cm-deep bed with inlet conditions of 100°C and 0.3 m/s.

$$V_{dz} = \frac{h}{t_{top}} \quad (6)$$

where h is the bed depth and V_{dz} is 2.2 mm/min for the conditions used for the data in Figure 3. Over the range of bed conditions, the drying zone velocities ranged from 1 to 10 mm/min and varied with the rate of drying.

The bottom of the drying zone reaches the top of the bed at t_{end} (Fig. 3). Therefore, the width of the drying zone (W_{dz}) can be expressed as

$$W_{dz} = V_{dz} \cdot (t_{end} - t_{top}) \quad (7)$$

The drying zone width varied from 0.13 to 0.18 m and was narrower with increasing temperature and decreasing gas velocity.

Model for bed drying

The lines in Figure 5 show results from the bed model overlaid on the experimental hemlock bed drying data. Initially, the model predicted drying that was too fast. This was attributed to channeling in the bed observed during the experiments, and a channeling factor was added to the model and set to 30 percent. The differences between drying time to 12 percent moisture content between the model and experiment ranged from −22 to +12 percent, with an average of ±3.4 percent. The model also predicts the shape of the drying curves, with pseudo r^2 values for any given simulation ranging from 0.84 to 1.00. The pseudo r^2 is used because the model and data are not linear and the value is only an estimate of the true r^2. The deep bed model also predicted a drying zone width of 0.11 to 0.18 m, in good agreement with the range estimated from the experimental data (0.13 to 0.18 m).

There is considerable moisture content variability in the bed when the final desired average moisture content reached. This is demonstrated in the model results (Fig. 6) that show as high as 50 percent moisture content in the upper layers and almost 0 percent in much of the lower portion at the end of drying, when the average bed moisture content is 7 percent. This suggests that mixing or a two-or-more-stage conveyer dryer might be needed to reduce moisture variability. The first stage would be slightly deeper than the drying zone width and operated until the drying zone reached the bed surface. This would avoid severe overdrying of the lower portion while maintaining thermal efficiency. The material would then be mixed and fed to another stage. The second or subsequent stages could be somewhat deeper because the width of the drying zone will increase if the concentration of wet material is less.

The deep bed drying model can predict the drying for Douglas-fir of the same shape and size (Fig. 7) using the thin-layer model for hemlock (Eq. 5). The fit is good, with a pseudo r^2 of 0.99 at both 100°C and 150°C. The lack of a difference in the bed drying characteristics of these two species is partly because a portion of bed drying is controlled by the saturation of the drying air and possibly because they have a similar specific gravity as well as particle size and shape.

With a deep bed drying model, the drying time in a fixed bed can be predicted given the initial moisture content and the inlet temperature, gas velocity, and humidity. Alternatively, the temperature and gas velocity required to dry in a given time could be determined. This is significant for determining the size of the dryer needed to process a certain amount of biomass. With a little extra calculation, the designer could determine the energy requirements for a dryer and size of the burner as well.

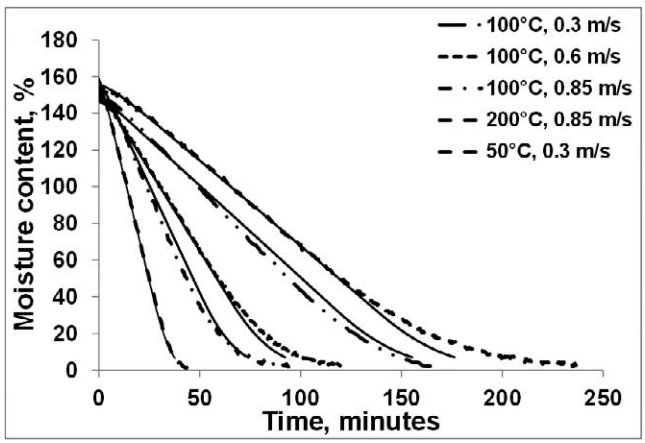

Figure 5.—Experimentally determined curves for moisture content versus time (broken lines) from a 23-cm-deep bed with model results (solid lines).

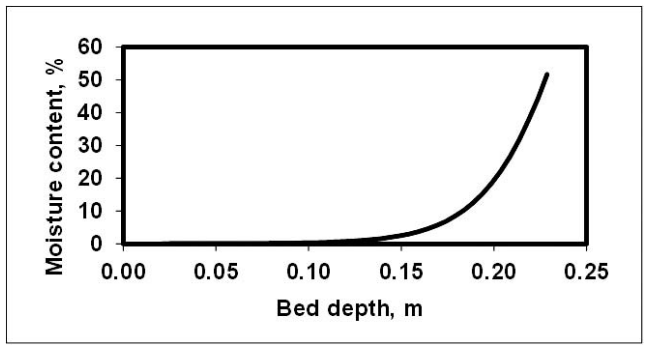

Figure 6.—Moisture content versus bed depth at the end of drying at 150°C. The average bed moisture content is 7 percent.

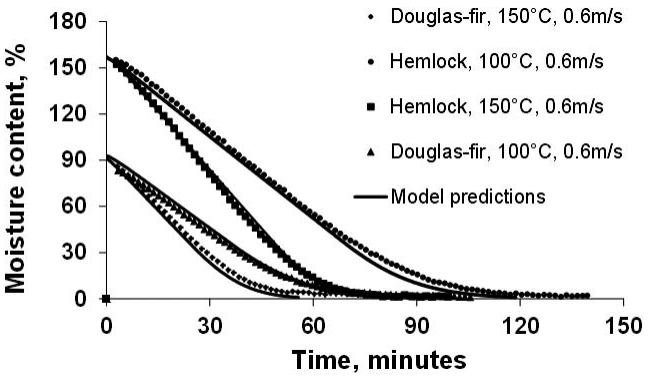

Figure 7.—Experimental and modeled curves for moisture content versus time for drying hemlock and Douglas-fir. The hemlock thin-layer model was used for both species.

The model also predicts the vertical moisture content profile within the dryer and may help designers determine the appropriate bed depth. In addition, the moisture variability leaving a dryer can be calculated, which may impact how downstream operations are performed. A designer would want the bed to be deep enough to contain the drying zone for most of the biomass residence time to maintain dryer efficiency. The model does not help the designer determine when channeling will occur or indicate when particle entrainment and carry over will occur.

Conclusions

The drying characteristics of wood particles can be measured by passing air through a thin layer of particles and obtaining the relationship of moisture content versus time.

A simple, one-parameter Newton model can describe the thin-layer drying in a fixed bed. The parameter is affected by temperature and air velocity. The Newton model developed for hemlock particles also works well for Douglas-fir particles. Further work is needed to determine the effects of size and shape on the model parameters.

A thin-layer drying model can be used in a deep bed model to predict the bed behavior at various drying temperatures and air velocities. This was demonstrated by experimentally developing thin-layer drying curves at temperatures from 50°C to 200°C and velocities from 0.3 to 0.9 m/s in a 1.3-cm-deep bed. The model was then used to predict the behavior in a deep bed and was experimentally verified.

A drying zone ranging from 0.13 to 0.18 m in depth occurs when drying hemlock particles. This was observed based on bed temperatures taken at different bed depths and was predicted by the deep bed model. An industrial dryer needs to be designed with a bed deep enough to fully contain the drying zone to maximize the efficiency of the dryer. The drying zone moves upward as drying proceeds, with the velocity and width of the drying zone being affected by the temperature and velocity of the drying air.

The material in an industrial dryer needs to be mixed, or a dryer needs to be designed with stages to avoid having very dry material at the bottom of the bed and very wet material at the top of the bed at the end of drying. Channeling air through the fixed bed may pose a problem for dryer efficiency in deep bed drying.

Literature Cited

ASTM International. 2007. Standard test methods for direct moisture content measurement of wood and wood-base materials. ASTM D4442-07. ASTM International, West Conshohocken, Pennsylvania.

Cui, H. and J. R. Grace. 2008 Spouting of biomass particles: A review. *Bioresour. Technol*. 99:4008–4020.

Ertekin, C. and O. Yaldiz. 2004. Drying of eggplant and selection of a suitable thin layer drying model. *J. Food Eng*. 63(3):349–359.

Gigler, J. K., W. K. P. van Loon, and M. M. Vissers. 2000. Forced convective drying of willow chips. *Biomass Bioenergy* 19:259–270.

Henderson, S. M. and S. Pablis. 1962. Grain drying theory, IV. The effect of airflow rate on drying index. *J. Agric. Eng. Res*. 7(2):85–89.

Jackson, S. W., T. G. Rials, A. M. Taylor, J. G. Bozell, and K. M. Norris. 2010. Wood2Energy: A state of the science and technology report. University of Tennessee, Knoxville.

Milota, M. R. and J. B. Wilson. 1990. Engineering analysis of the drying of wood particles in a fluidized bed. *Wood Fiber Sci*. 22(2):193–203.

Mujumdar, A. S. 2007. Handbook of Industrial Drying. CRC Press, Boca Raton, Florida. 1,280 pp.

Otwell, L. P., M. E. Hittmeier, U. Hooda, H. Yan, and S. Banerjee. 2000. HAPs release from wood drying. *Environ. Sci. Technol*. 34:2280–2283.

Paulsen, M. R. and T. L. Thompson. 1973. Drying endysus of grain sorghum. *Trans. ASAE* 16:537–540.

Phanphanich, M. and S. Mani. 2009. Drying characteristics of pine forest residues. *BioResources* 5(1):108–121.

Roos, C. J. 2008. Biomass drying and dewatering for clean heat & power. WSUEEP08-015. Washington State University Extension Energy Program, Olympia.

Siau, J. 1984. Transport Processes in Wood. Springer-Verlag, Berlin. 245 pp.

Skaar, C. 1998. Wood-Water Relations. Springer-Verlag, Berlin. 283 pp.

US Department of Agriculture. 2010. Wood handbook—Wood as an engineering material. General Technical Report FPL-GTR-190. USDA Forest Service, Forest Products Laboratory, Madison, Wisconsin. 508 pp.

Verma, L. R., R. A. Bucklin, J. B. Endan, and F. T. Wratten. 1985. Effects of drying air parameters on rice drying models. *Trans. ASAE* 28(1):296–301.

Wang, C. Y. and R. P. Singh. 1978. A single layer drying equation for rough rice. Technical Paper 78-3001. American Society of Agricultural Sciences Summer Meeting, June 27–30, 1978, Logan, Utah.

Wang, Z. H. and G. Chen. 1999. Heat and mass transfer in fixed-bed drying. *Chem. Eng. Sci*. 54:4233–4243.

Westerman, P. W., G. M. White, and I. J. Ross. 1973. Relative humidity effect on the high-temperature drying of shelled corn. *Trans. ASAE* 16(6):1136–1139.

Yang, H. 2012. Modeling the fixed bed drying characteristics of biomass particles. Master's thesis. Oregon State University, Corvallis. 123 pp.

Yrjölä, J. and J. J. Saastamoi. 2002. Modelling and practical operation results of a dryer for wood chips. *Drying Technol*. 20(6):1077–1099.